International Journal of ENGINE RESEARCH

Standard Article

International J of Engine Research
1–13

DOI: 10.1177/1468087420967873
journals.sagepub.com/home/jer
SAGE

Investigation of ammonia and hydrogen as CO2-free fuels for heavy duty engines using a high pressure dual fuel combustion process

Stephanie Frankl, Stephan Gleis, Stephan Karmann, Maximilian Prager and Georg Wachtmeister

Abstract

This work is a numerical study of the use of ammonia and hydrogen in a high-pressure-dual-fuel (HPDF) combustion. The main fuels (hydrogen and ammonia) are direct injected and ignited by a small amount of direct injected pilot fuel. The fuels are injected using a dual fuel injector from Woodward L'Orange, which can induce two fuels independently at high pressures up to 1800 bar for the pilot fuel and maximum 500 bar for the main. The numerical CFD-model gets validated for of hydrogen-HPDF with experimental data. Due to safety issues at the test rig it was not possible to use ammonia in the experiments, so it is modelled using the numerical model. It is assumed that the CFD-model also gives qualitative correct results for the use of ammonia as main fuel, so a parameter study of ammonia-HPDF is made.

The results for the hydrogen-HPDF show, that hydrogen can be used in the engine without any further modifications. The combustion is very stable, and the hydrogen ignites almost immediately when it enters the combustion chamber. The results of the ammonia combustion indicate, that the HPDF combustion mode can handle ammonia effectively. It seems beneficial to inject the ammonia at higher pressures than hydrogen. Also pre-heating the ammonia can increase the combustion efficiency.

Keywords

Dual fuel, hydrogen, ammonia, CFD-simulation, high pressure dual fuel

Date received: 28 July 2020; accepted: 21 September 2020

Introduction

In times of climate change, marine propulsion systems must also increasingly reduce climate-damaging emissions. This requires innovative approaches. One way to reduce CO2 emissions in internal combustion engines is to substitute diesel through natural gas but this often goes hand in hand with methane emissions from incomplete combustion, especially when using premixed lean gas combustion. Methane is 28 times more harmful to the climate than CO2.[1] A method to lower the methane emissions significantly is the use of a high-pressure direct injection of the gas into the combustion chamber.[2] This gas is ignited by a small amount of pilot fuel, usually diesel and burns in diffusive combustion mode. The direct injection of the gas and the diffusive combustion enable significantly higher compression ratios and better efficiencies than premixed gas engines.

Several research groups in Canada, Japan and Europe have been working on the topic and have been able to demonstrate that methane emissions can be significantly reduced with the combustion process compared to classic natural gas engines.[3–7] Nevertheless, the combustion of natural gas still produces CO2 as combustion product. Therefor there is a need for fuels that do not contain carbon in their molecular structure. Two promising fuels – which fulfil this requirement and therefore do not produce CO2 emissions – are hydrogen and ammonia. Table 1 gives an overview over Hydrogen and Ammonia compared to methane.

In a 4-year, publicly funded project, a dual-fuel injector was developed that is capable of injecting other fuels in addition to natural gas next to the auto igniting pilot fuel.[11,12] This injector has been used experimentally for

Institute of Internal Combustion Engines, Technical University of Munich, Munich, Germany

Corresponding author:
Stephanie Frankl, Institute of Internal Combustion Engines, Technical University of Munich, Schragenhofstr. 31, Munich 80992, Germany.
Email: stephanie.frankl@tum.de

Table 1. Fuel properties using data from.[8–10]

	Hydrogen	Ammonia	Methane
Critical temperature	33.145 K	405.4 K	190.6 K
Critical pressure	12.964 bar	113.33 bar	46.1 bar
Normal boiling point	20.369 K	239.823 K	111.2 K
Phase state at 500 bar and 350 K	Supercritical	Liquid	Supercritical
LHV [MJ/kg]	120	18.8	50.0
Flammability limits (λ)	0.14–10.0	0.71–1.58	0.59–2.0
Adidabatic flame temperature	2110 K	1800 K	1950 K

the above mentioned methane-diesel and methanol-diesel dual fuel combustion in a full optical accessible internal combustion engine in previous works.[13,14] From the experiments a numerical CFD-model was developed and validated.[15,16] A derived model is used in this study to investigate the substitution of methane through hydrogen or ammonia in order to find out whether these fuels are suitable for HPDF-engines.

Hydrogen as fuel

Hydrogen is the simplest element. Combined with oxygen it reacts to water. The stored energy of hydrogen can be used through combustion with an oxygenator or electro chemical reaction in a fuel cell. Fuel cells require a very high purity of hydrogen (99.97%, ISO14687: 2019[17]) whereas combustion engines can cope with lower purities of hydrogen. Hydrogen already has a long history as standard fuel for rocket engines, especially lower and middle stages as the Vulcan engine since over 30 years, usually used in liquid state together with liquid oxygen.[18]

However, in internal combustion engines also has been research.[19] For example BMW built up one of the first cars with an internal combustion engine running on hydrogen in 2006.[20] There was also research for stationary hydrogen gas engines in Austria.[21] But the use in premixed Otto-combustion process is very challenging because of knocking or ignition because of small amounts of lubrication oil in the combustion chamber. The direct injection with diffusive combustion do not show these phonomena. Rottengruber et al. burned hydrogen in a medium bore diesel engine in the early 2000 using direct injection and auto ignition of the fuel.[22] They had to heat up the intake air to about 70°C to enable a stable combustion process – which reduced the efficiency of the engine.

Nowadays the majority of hydrogen is produced via steam reformation from fossil natural gas (grey hydrogen). If hydrogen is produced using carbon capture, it is referred as blue hydrogen. However, it can also be produced by electrolysis using power from regenerative energies like wind, water or solar plants – which makes it interesting as climate-friendly future fuel (green hydrogen).[23,24]

The easy hydrogen is to produce, the hard the storage of hydrogen is. Usually it is stored either in gaseous state at high pressures, or as cryogenic liquid. Both ways require a great amount of energy to be realized. Gaseous hydrogen has a comparably low volumetric energy content, which limits the range of the vehicles or ships due to huge tank sizes. In liquid state, the volumetric energy content is better, but the liquid state of hydrogen requires very low storage temperatures of 20K – which is also a big challenge, especially on vehicles or ships.

Further approaches to hydrogen storage are metal hydrides as used in the type 212 submarine used by the Italian military. The disadvantages of this storage method are the high weight and the very slow removal of the hydrogen. Therefor the chemical storage of hydrogen in heavier atoms is interesting. One example is methane, another – which is not based on carbon – to realize this is Ammonia.

Ammonia as fuel

Almost 50% of the world's hydrogen production is used for ammonia production.[25] Most of the worldwide ammonia production is used for agriculture and for this use transported and stored all around the world. In liquid state, the volumetric hydrogen-density in ammonia is higher than in liquid hydrogen[26] so it is often considered as hydrogen carrier. Because of the already existing infrastructure for transport and storage of ammonia, the direct use as fuel becomes interesting. It can be produced by using green hydrogen with energy from renewable sources like wind, water or solar plants. The thermo-catalysis of ammonia back to hydrogen requires a high amount of energy, so the idea of using ammonia directly as fuel is interesting.[26]

Ammonia already has history as an engine fuel.[27] In times of the Second World War, Belgium used ammonia as fuel for buses in public transportation due to shortage of diesel fuel.[28] Also in California, US, there were cars running on ammonia due to shortage in fossil fuels. The US military conducted several studies on ammonia as fuel in order to be more fuel independent.[29] Ammonia is also necessary for the selective catalytic reduction for meeting the NOx-emission regulations for diesel engines and in form of urea already aboard of many internal combustion systems. Even in low concentrations, ammonia is toxic and very harmful to the

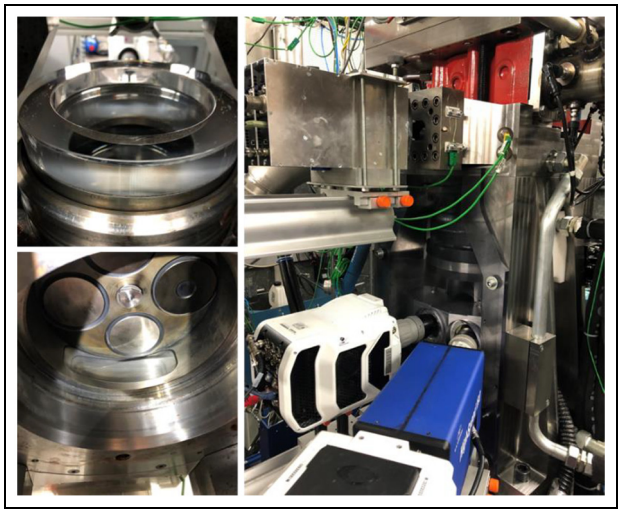

Figure 1. The optical engine. Small picture up left is the glass piston bowl, in the lower left picture the cylinder head with the injector from below; in the middle the lateral window can be seen. The picture on the right shows the arrangement of the two cameras one with the image intensifier (blue).

environment, so special safety precautions must be taken when handling it.[30]

Methodology

Structure of the HPDF-combustion

In this work, the fuels are injected using a dual fuel injector from Woodward L'Orange, which can induce two fuels independently at high pressures up to 1800 bar for the pilot fuel and maximum 500 bar for the main fuel.[12] In the HPDF combustion, the two fuels can be injected individually and independent from each other. This enables premixing, staged combustion as well as diffusive combustion.

The used numerical model is validated using data from the optical accessible single cylinder test engine described in Gleis et al.[13] and Frankl and Gleis.[15] Developed for methane-diesel dual fuel it is extended for the fuel combinations hydrogen/diesel and ammonia/diesel in this work. The experimental setup as well as the numerical model are described in the following.

Experimental setup

The numerical model used in this work is derived from previous works of the authors using the commercial software package CONVERGE CFD.[31] The basis of this model is a full optical accessible single cylinder engine (see Figure 1) in the Bowditch-design.[32] It is derived from a marine MTU 4000 Diesel engine, with 170 mm bore and 210 mm stroke. It has a flat cylinder head with valve masking for swirl generation. To have best optical access the piston bowl is cylindrical shaped. The used compression ratio is 17. The inlet valves use a

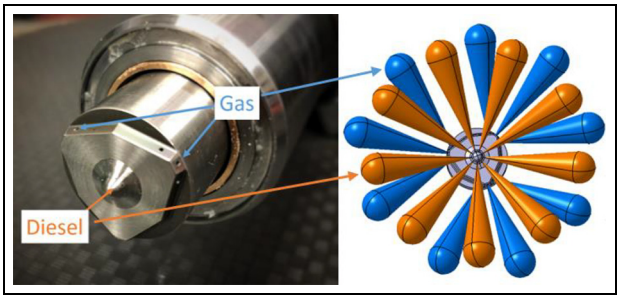

Figure 2. Image of the injector Nozzle and spray arrangement.

Miller timing, to intensify the swirl at the injection point.

The engine is equipped with the Woodward L'Orange HPDF dual fuel injector.[12] The Injector is centrally mounted in the cylinder head. The injector nozzle has nine holes for main fuel and nine holes for the diesel pilot injection (Figure 2). The diesel and the gas injection work independently from each other. For the experiments used in this work, injection pressures for the main fuel are 300 bar and 500 bar, for the diesel side 1000 bar and 1200 bar.[14]

The engine is equipped with two optical accesses; one lateral access where a LED-flash lamp is placed for illumination of the liquid spray phases, and a glass insert in a prolonged piston. Via a mirror and a beam splitter two cameras simultaneously record the flame luminosity and the OH-chemiluminescence signal.

The engine is built for maximum cylinder pressures of 300 bar and is run at 750 rpm max. The cooling of the optical piston is mainly through air ventilation, so in order not to overheat the glass, the maximum of fired cycles in a row is limited to 70. A more detailed description of the experimental setup can be found in.[13,14]

Experiments were made using methane and hydrogen as main fuel and diesel as pilot fuel ignition source.[14] Due to safety issues at the test rig it was not yet possible to use ammonia in the experiments so it is only modelled using the numerical model described below.

Numerical model

A numerical model was build up and validated using data for Methane-Diesel HPDF combustion in Frankl and Gleis[15] and Frankl et al.[16] using the commercial software Converge CFD. In this work, the model is validated with hydrogen HPDF-combustion experiments, afterwards further reduced, and simplified to a 40°-sector to reduce the computational effort of the parameter variation study.

The 120° and the 40° models are initialized with a flow-field from a full-scale simulation model, which is initialized on experimental measured data. How the models are related to each other is shown in Figure 3.

For the initial conditions for sector models, a full-scale charge-exchange (without combustion) simulation

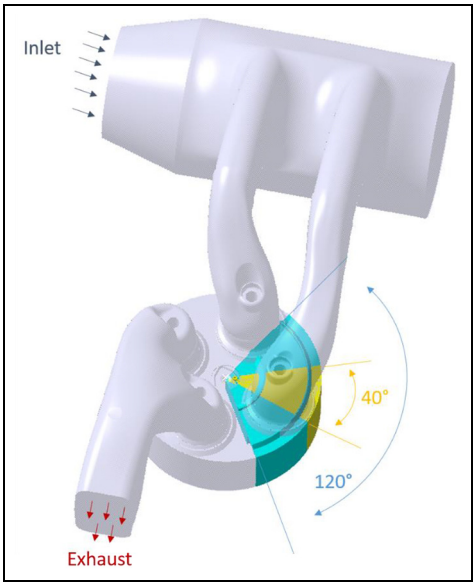

Figure 3. Simulation domains for generating the initial conditions, the 120° sector and the simplified 40° sector model.

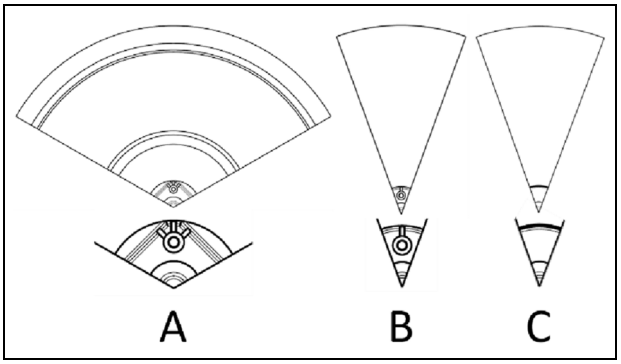

Figure 4. Top view of the used sector models for the numerical simulations including a closer view of the injector part: (a) the 120° model including gasnozzle geometry, (b) 40° model including gasnozzle, and (c) 40° model for liquid fuel injection only.

is made consisting of two whole cycles. Its boundaries are taken from measurements of the optical engine; the intake air temperature and pressure as well as the exhaust pressure and temperature. The flow field is initialized with a start solution with similar boundary conditions from previous work so using the second simulated cycle for combustion initialization is sufficient.

The flow field is described using the Reynolds-averaged-Navier-Stokes equations with the k-ε-RNG turbulence model and the Redlich-Kwong equation of state. The liquid spray injection is modelled using Lagrangian particles, with the Kevin-Helmholtz-Rayleigh-Taylor (KHRT) breakup model and the 'no time counter' (NTC) method for droplet collision. The injection rate is given by injection rate measurements of the diesel side of the injector. For a gaseous main fuel injection, a mass flow boundary is used. For this purpose, the lower part of the gas side of the injector nozzle is included into the model. For the liquid ammonia injection the liquid spray is also modelled using Lagrangian particles, the KHRT model and NTC collision.

The combustion is calculated using the SAGE Detailed Chemical Kinetics Solver with reaction mechanism resulting from a combination of the GRI3.0[33] for methane and the Chalmers53 n-heptane mechanisms. The Chalmers 53 has been giving good results for methane-diesel HPDF in[34,35] and the GRI3.0 is validated in literature – giving satisfying results for the laminar burning velocity in ammonia combustion.[10,36]

The hexagonal grid is of 1x1x1mm base size using fixed embeddings for the wall boundaries and liquid injection as well as adaptive mesh refinement for the velocity and temperature gradients. The edge length of the resulting minimum cell size in the domain is 0.0625 mm. Exemplary images of the grid at two crank angles can be found in the appendix.

Further reduction of the numerical model

In order to reduce the computational effort the 120° sector model was reduced to a 40° sector model. The gas injector is modified to have just one hole for the gas injection instead of three (see Figure 4). This changes the flow conditions in the injector sack hole and has an influence on the emerging fuel jets. So, a comparison of the results of the 120° and the 40° of the same reference point was made and compared against experimental results to examine the influence of the 40° simplifications.

Figure 5 shows an exemplary comparison between the heat release rate (HRR) from the experiment, the 120° sector (A) and the 40° sector model (B) for a methane-diesel HPDF case. As can be seen, the diesel combustion is almost identical for the 120° and the 40° sector and very close to the measured data.

For the main fuel combustion there is a slightly later start of ignition and a higher premixed peak. This is a result of the different flow conditions in the nozzle sack-hole because of the reduction from three holes in the 120° case to one hole in the 40° case. A second source of inaccuracy is the fact, that the 'outer' gas jets in the 40° sector are assumed as orientated to the rotation centre, which is not correct (see Figure 5) – so there arises a deviation from the angle for six of the nine jets where they hit the pilot diesel. The ignition of the middle gas jet is nevertheless very similar to the ignition in the 40° sector, as can be seen in the lower part of Figure 5. For a better comparison, the soot luminescence image is plotted next to the simulation. From the end of the injection, the HRR curves show a very similar behaviour for both sectors.

For the validation with the experimental HPFD-combustion data, the 120° is chosen because of the higher accuracy. For the following comparisons

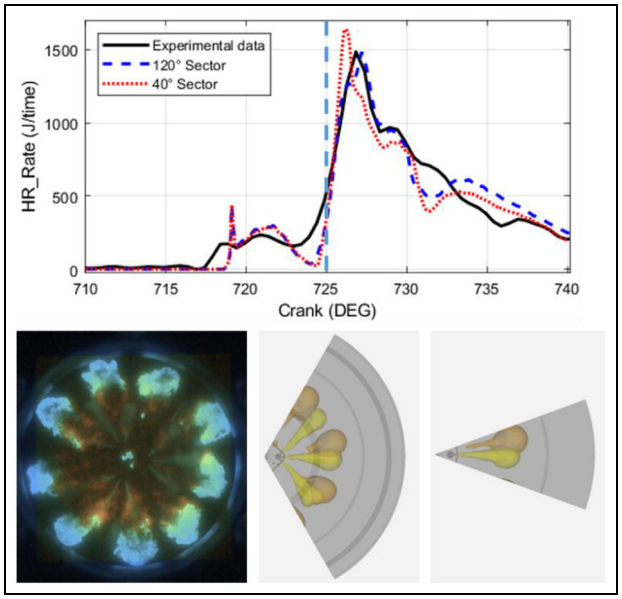

Figure 5. Heat release rate of the 120° and 40° sector models compared to the experimental measurement (average of 10 cycles) and qualitative comparison of the gas ignition at 725°CA (20th cycle in experiment, 120° sector and 40° sector models).

between hydrogen and ammonia HPDF combustion as well as the understanding of the qualitative influence of parameters on ammonia ignition, the 40° sector is a sufficient choice.

Hydrogen high pressure dual fuel combustion

Table 2 gives an overview about the reference hydrogen HPDF-combustion point. The exact start of injection (SOI) for both fuels are taken from the high-speed images. In the following, the results of the hydrogen HPDF simulations are shown and compared to the experimental data.

The HPDF-combustion is extraordinary stable compared to premixed Dual-Fuel combustion. Figure 6 shows the variance of the cycle fluctuations in the measured pressure curves of diffusive hydrogen, methane and diesel combustion of the same load in the optical engine compared to a premixed dual fuel combustion (methane-hydrogen mix with pilot ignition) in the same engine.

It can be seen that from 356° to 360,7°CA the cylinder pressure variance

$$Var = \frac{\sum (p - p_{mean})^2}{(n-1)}$$

(p cylinder pressure, n number of cycles) of the diffusive combustion cases is very similar and lies between 0.7 and 3.6. This is the time range, where the pilot combustion takes place. For the diesel case, the variance stays at this level for the main combustion. For the methane HPDF combustion, the variance has a peak 364.1°CA.

Table 2. Data of the reference point.

Inlet pressure	6.5 bar
Exhaust pressure	5.2 bar
Main fuel	500 bar
Pilot fuel	1200 bar
Fuel injection temperature	380 K
SOIPilot	715.5°CA
SOI main fuel	720°CA

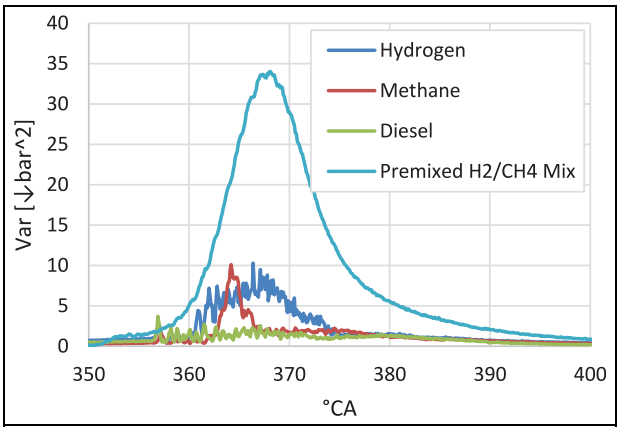

Figure 6. Variance of in-cylinder pressure for hydrogen and methane HPDF and diesel combustion with pilot injection as pre-injection.

This is where the ignition of the gas jets happens. Due to inhomogeneity in the jet penetration, sometimes a jet ignites earlier or later than others do. When all methane jets are enflamed, the variance level lies just a little bit above the diesel-only combustion.

The variance of the hydrogen combustion stays comparable high for the whole time of the main combustion and returns to similar values as in the diesel or methane case after the injection has ended at 372°CA. To eliminate the variation factor, the images of the hydrogen HPDF experiments are averaged over 25 cycles for the comparison with the simulation results.

Figure 7 shows the comparison of the pressure curves and the HRR from experiment and CFD-simulation. The ignition delay time of the diesel injection in the simulation is about 1°CA longer than in the experiment. Following that, the hydrogen ignition is also 1° later than in the experiment. The simulation nevertheless overestimates the pressure curve with a maximum deviation of 9% at top dead centre (TDC).

Figure 8 shows the OH*chemiluminescence images compared to the OH-isosurfaces in the simulation results at the same crank angle. At 362°CA the ignition of the hydrogen jets can be detected. The hydrogen ignites immediately when it hits the hot pilot combustion products, very close to the injector. It can be seen that the pilot combustion rotates counter clockwise because of the engines swirl. Therefore, the pilot jets are between the gas jets when the gas injection starts. The

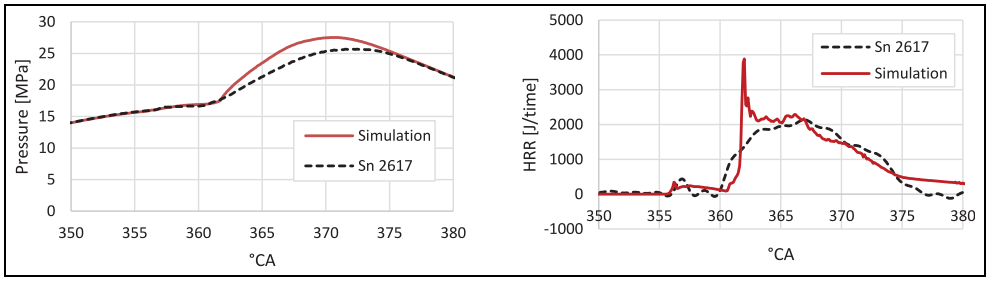

Figure 7. Pressure curves and heat release rates from experiment and simulation.

simulation shows this effect very well. At 364°CA the hydrogen has reached the cylinder bowl and the jets are redirected along the wall. The burning areas become wider and are blown away by the swirl in a counter clockwise direction.

Looking at the flame lift-off length at 364° and 366°CA in the simulation, the OH-production seems to start immediately when the hydrogen enters the combustion chamber. This effect can also be detected in the OH*-chemiluminescence images. As shown above (see Table 1) Hydrogen has very wide flammability limits and a very high laminar flame speed. Although the hydrogen jet enters the chamber at supersonic speed, the flame is able to spread upstream in the thin shear layer between jet and surrounding air.

Also for a fuel with very wide flammability limits like hydrogen, the heat release with HPDF combustion is limited by mixing of air and fuel, which can be seen in the broadening of the OH*-chemiluminescence signal, as well as in the OH-isosurfaces in the simulation. Some of the hydrogen gathers at the piston bowl walls, which reacts after the injection has stopped (from 371.5°CA on – not shown, but visible in the HRR in Figure 7).

The simulation shows deviations from the experiment especially in the HRR and pressure curve whereas the 3D results show good agreement with the experimental images. For the diesel injection, it is very difficult to match the experimental data for various reasons. First, the injector used, is a prototype-injector for research purposes. The diesel side of the injector is designed for full load diesel combustion. For the smallest quantities used (about 1%–2% of the energy content), the needle is operated in the ballistic range. In the needle seat there is a small geometric deviance from manufacturing of the prototype nozzle used, leading to an uneven opening cross section.

This is visible in the jet pattern of the pilot spray. Some of the diesel jets do almost not penetrate into the combustion chamber as shown in the left picture in Figure 9. Therefore, also the hot combustion products that work as ignition source for the hydrogen jets are not spread evenly (right picture series in Figure 9). Some of the propagating jets therefor ignite earlier than others – this effect is not great but it explains the differences in the HRR at the beginning of the hydrogen combustion.

The simulation model used in this work is not able to reproduce this asymmetry of the pilot combustion because of the assumed rotational symmetry. It would be necessary to extend the model to the complete combustion chamber geometry and to carry out a simulation of the internal nozzle flow of the diesel side of the injector – including the manufacturing deviance – in order to in order to reproduce these effects in the CFD. This would have led to extraordinary high computational cost.

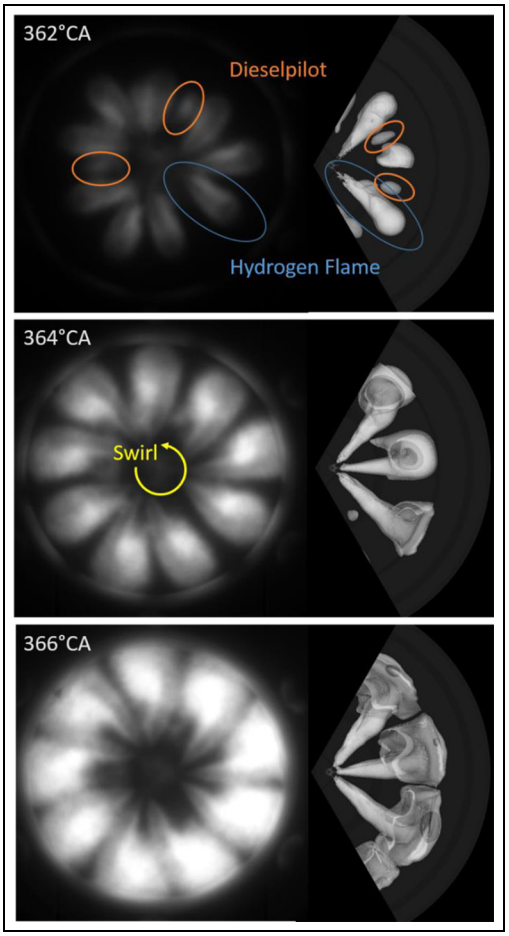

Figure 8. Comparison of the OH*-chemiluminescence image on the lefts (average of 26 cycles) and the OH-isosurfaces (0.001% mass) in the simulation in the right at the beginning of the hydrogen combustion.

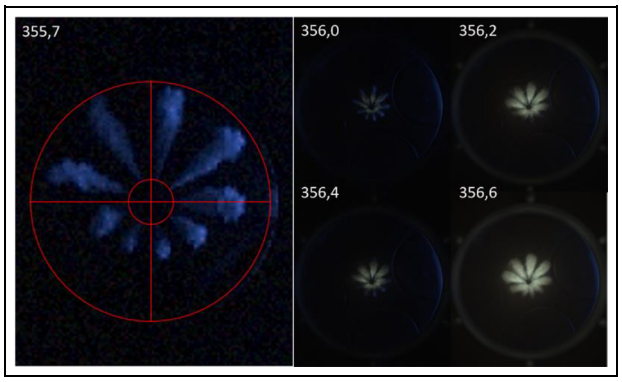

Figure 9. MIE-imaging of the diesel pilot spray (left) and flame luminosity pictures of the ignition pilot diesel (right).

There is a further uncertainty regarding the injection rates used for the hydrogen injection. The injected mass per firing is measured using a Coriolis mass flow meter. However, for safety reasons, the injection rates were measured using an injection analyser with nitrogen at constant back pressure. The curves were converted to hydrogen using material values. However, the variable combustion chamber pressure can influence both the opening and closing behaviour of the nozzle needle and the flow through the nozzle hole – which changes the effective mass flow and therefor the HRR.

Apart from the relatively small and easily explainable deviations in the global curves, the model shows a good agreement with the optical images of hydrogen combustion. Because of the fact, that the numerical model, which was initially developed for methane-HPDF, gives also good results for hydrogen as main fuel, it is assumed to also produce reasonable results for other fuel-combinations.

In the following, the results of a numerical study for hydrogen and ammonia HPDF-combustion are presented.

Numerical study of hydrogen and ammonia HPDF

The compression end pressure for the numerical study is 90 bar. This is, because the study was performed before the experimental data was gained, and therefore based on the experiments published in Gleis et al.[13] and Frankl and Gleis.[15] The first hydrogen HPDF simulation was made in order to find out, if an engine process with hydrogen in HPFD combustion would be safe.

Table 3. Reference point conditions.

Main fuel	500 bar
Pilot fuel	1000 bar
Fuel injection temperature	350 K
SOIPilot	717.5°CA
SOI main fuel	721°CA
Cylinder pressure at 715°	90 bar

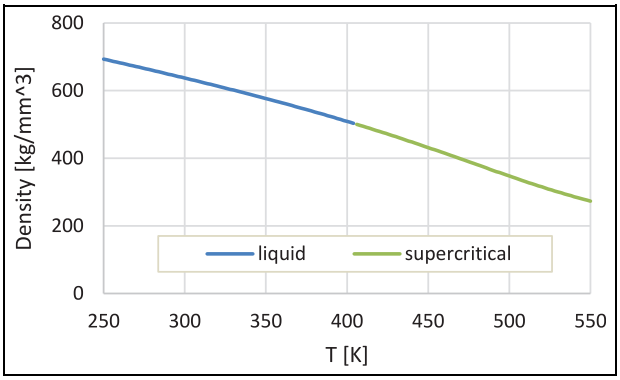

Figure 10. Fluid data of ammonia using data from.[37]

Comparison of hydrogen and ammonia combustion

The reference point for the numerical study is derived from the work in Frankl and Gleis.[15] The used parameter for the following simulation results are given in Table 3.

The simulations are initialized using a map-file for initializing the cylinder flow. The flow-field in the map file is validated with PIV-imaging from previous work.[13]

Unlike hydrogen, ammonia is known for its poor flammability – the auto ignition temperature is 903K compared to 833K for hydrogen. In the reference point conditions (ammonia at 500 bar, 350K), the ammonia is injected in liquid state as can be seen in Figure 10.[37] The model C from Figure 4 is used to simulate two liquid injections (pilot & fuel).

The vaporization of the ammonia additionally needs energy form the cylinder charge that is not available for ignition. Figure 11 shows the comparison of ammonia HPDF-combustion with hydrogen using the reference point timings. The heat release curves show, that the ignition of ammonia is delayed compared to hydrogen. The peak of the HRR occurs after the injection has

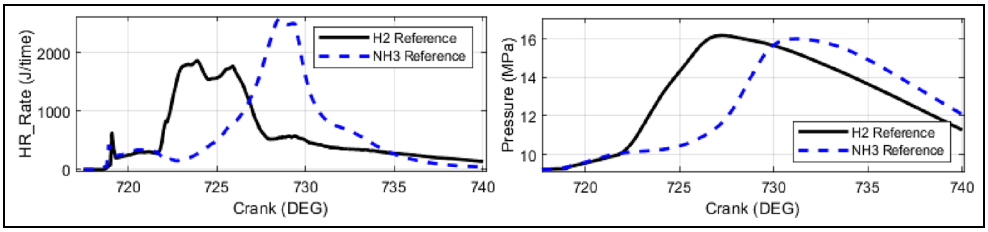

Figure 11. HRR and pressure of hydrogen and ammonia HPDF compared.

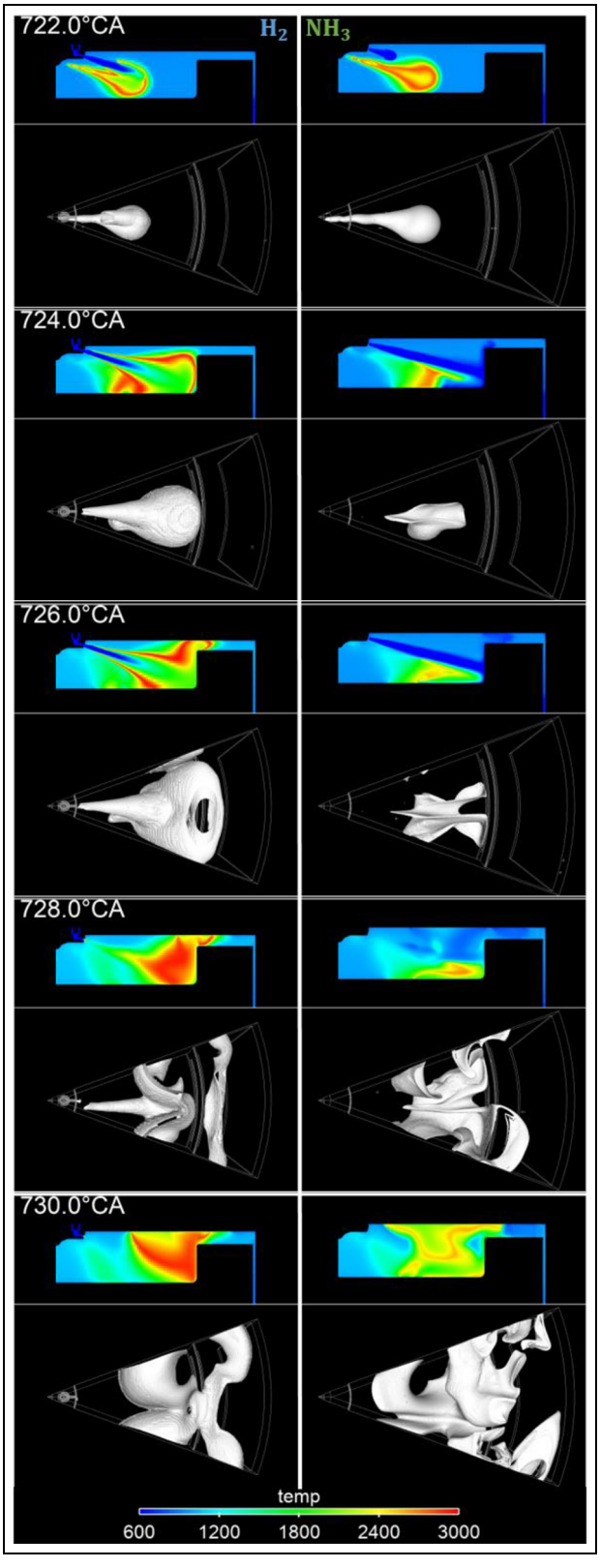

Figure 12. Topview of OH-Isosurface at 0.001% and Temperature in the $y = 0$ plane of the 40° Sector models of hydrogen (left) and ammonia.

already stopped. Nevertheless, the abrupt release generates a similar peak pressure as in hydrogen combustion.

In addition, the form of the HRR curve indicates a mainly premixed combustion, which can be confirmed by examining the 3D data shown in Figure 12. It shows an isosurface of OH as an indicator for flame and the temperature in the $y = 0$ cut plane. The lower injection is the pilot diesel, the upper the main injection.

It can be seen, that the hydrogen almost immediately ignites when it enters the combustion chamber because it directly hits the diesel combustion. This is reasonable as this has similar been shown in Figure 8. At 722°CA there is already a flame around the tip of the hydrogen jet. In the temperature image, it can be seen that the ammonia also hits the burning diesel flame but does not yet ignite.

At 724° the ammonia as well as the burning hydrogen jets hit the piston bowl wall. The ammonia jet has displaced the combustion products of the diesel towards the bottom of the piston bowl. Only a small amount of the ammonia is reacting with the surrounding air close to the piston bowl. The laminar flame speed of ammonia is very low, and combined with the small flammability range the combustion propagates very slowly. The hydrogen also has displaced the pilot combustion products to the bottom of the bowl but a flame surrounds the hydrogen jet.

At 726° it can be seen, that in the hydrogen case, the flame blocks the hydrogen from penetrate into the crushing gap, but the ammonia almost reaches the cylinder wall. The OH surface in the ammonia case starts to grow from the bottom of the piston bowl into the areas where the ammonia jet is redirected by the piston bowl walls.

From 728° to 730°CA a much wrinkled flame develops and enflames the ammonia-air mixture. This can also be seen in the high peak in the HRR in Figure 11. In the hydrogen case, most of the combustion at this time has almost finished at 728° and the hot products are distributed in the combustion chamber. The adiabatic flame temperature of ammonia is very low compared to other fuels as methane or hydrogen, so the temperature rise through the ammonia combustion itself in the beginning is very low which in turn also does not promote faster processing of the fuel.

Parameter variation study of ammonia combustion

In the parameter variation study, the injection timing for ammonia as well as the injected mass is the same for all cases. The nozzle-hole diameter was adjusted in order to reach the desired injection pressures.

As studies in literature show, the equivalence ratio and the pressure have an influence on the ignition delay times.[38,39] In addition, as shown above, the autoignition temperature of ammonia is at 903K, which is very high compared to hydrogen with 833K. A study changing the injection pressure was made at 400K injection temperature. The results are shown in Figure 13:

The ignition delay time of the ammonia combustion stays quite similar for all cases. However, the increase in the HRR gets steeper with raising pressure. This is

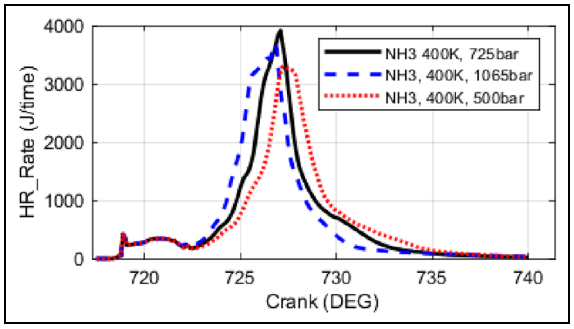

Figure 13. Heat release rates for the pressure variation study.

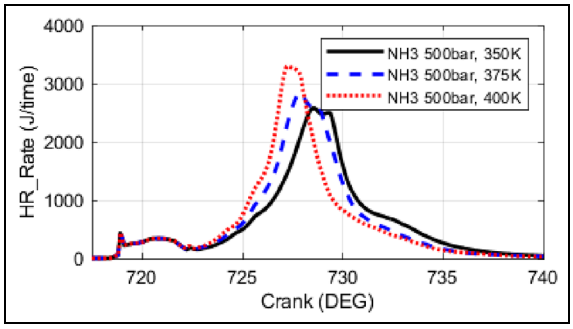

Figure 14. Heat release rate for temperature variation study.

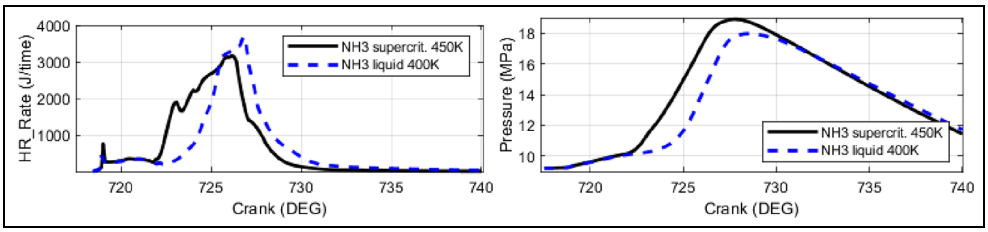

Figure 15. Influence of the phase state on the NH3-HPDF combustion.

probably due to the higher spray impulse and therefor better mixing of the ammonia with the surrounding air.

Mainly in the lower pressure cases, it can be seen, that the vaporization energy for ammonia is also quite high. A variation of the injection temperature was made to evaluate the influence of the liquid injection temperature on the heat release rate. Figure 14 shows the results of the HRR.

It can be clearly seen, that the ignition delay of the ammonia combustion is reduced with raising temperature. The lower energy content through colder injection temperatures need more time to heat up through the surrounding cylinder temperature.

The higher the fuel temperature, the higher is the resulting peak in the HRR. Liquid ammonia requires a lot of energy for vaporization. To evaluate the influence of the phase change a simulation with injection of supercritical ammonia was made. The ammonia phase changes to supercritical at 450K. The simulation used the same geometry as for hydrogen; keeping the mass flow rate constant, this results in an injection pressure of 1065 bar. In Figure 15 the result of this is shown against the NH3 liquid case at 1065 bar.

The HRR shows that the ignition starts almost immediately when the ammonia jet hits the pilot combustion products, similar to the hydrogen case. The peak in the HRR is now 0.2° bevor the EOI. The peak pressure in the supercritical case is also 10bar higher than in the liquid case and 0.6° earlier.

Looking at the OH concentration in Figure 16, it can be seen that, the tip of the jet in the supercritical case ignites when it hits the diesel combustion products whereas the liquid jet shoots just through it. The

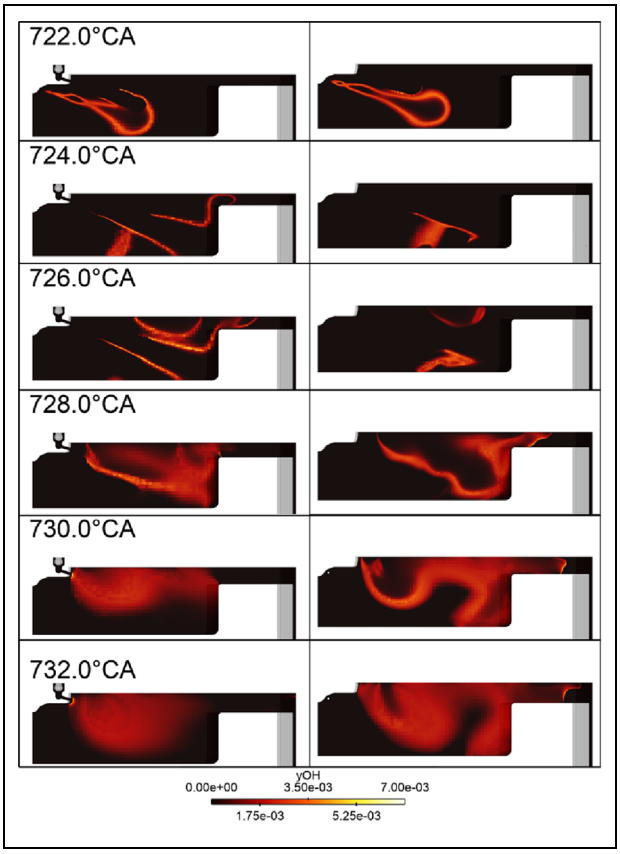

Figure 16. OH-Concentration in the supercritical (left) and liquid (right) cases.

supercritical case jets begin to burn at the sides of the flanks (726°CA). In the liquid case, the jets are redirected by the piston bowl before most of it reacts.

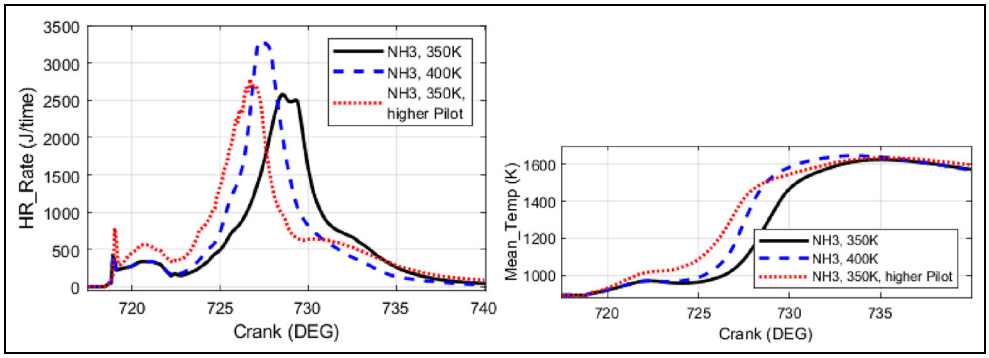

Figure 17. HRR and in-cylinder mean temperature of ammonia with a doubled pilot mass compared to the temperature variation cases.

Instead of increasing the temperature of the ammonia, one could also increase the temperature in the cylinder through a higher pilot diesel mass. Figure 17 shows the resulting HRR of a case with a doubled diesel pilot mass. It can be seen that because of the higher temperature in the combustion chamber at the start of the main injection, the ammonia ignites earlier. Nevertheless, the afterburning is comparable to the case with the standard pilot mass whereas the case with the higher ammonia temperature finishes earlier.

Discussion of the results

The comparison between hydrogen and ammonia combustion shows, that without any further actions, the ignition of ammonia is delayed. Reasons for this are its low flammability range, a high vaporization energy and high ignition temperature. The combustion is mainly premixed and shows a wrinkled flame propagation. To examine influences a parameter study of the ammonia combustion was made.

A higher injection pressure improves the mixing, and therefor the HRR is shifted early. Nevertheless, the used high pressures require a lot of energy for compressing the fuel and places high demands on the injection system. A easier way to enhance the combustion, which is already state of the art for ship engines running with heavy fuel oil, is preheating of the ammonia. A higher injection temperature of the ammonia leads to faster vaporization and better mixing. Nevertheless, the conversion of the fuel still happens suddenly, a shifting of the fuel injection to earlier times does not seem to make sense because of the expected high pressure rise gradients.

To examine the influence of the vaporization energy the ammonia was heated up to supercritical state. Because of the very high resulting injection pressure this is more of a theoretical case. But it shows that the shape of the curve approximates that of the heat release rate of hydrogen.

The easiest way to improve the ammonia ignition seems to be an increased amount of pilot fuel mass. Regarding the decarburization of the engine there has to be a trade-off between efficiency of the ammonia combustion and CO2 production of the used pilot fuel.

Conclusion

In the first part of this study a short overview about hydrogen and ammonia as fuels is given. The experimental and numerical setups of this study are presented. A 40° sector model is derived from the 120° model. A comparison of experiment, 120° sector and 40° sector is shown for a representative methane-HPDF-combustion and shows good agreement with the experimental results.

It is shown that the numerical model which was previously developed for methane is also capable of handling hydrogen as main fuel. The results of the 120° sector model are validated with experimental data and a comparison with OH*-chemiluminescence is made. The results show a good agreement of simulation and experiment.

The 40° model is used to simulate variations of hydrogen and ammonia HPDF combustion.

The simulation results show, that the hydrogen flame burns very close to the injector. This could cause problems for the long-term durability of the injection system because of the very high flame temperatures close to the injector geometry. Hydrogen burns almost exclusively diffusively and is very easy to ignite. Probably even smaller amounts of pilot diesel mass could be possible – which would further reduce the CO2 emissions of the engine. In this case, the injector would be the limiting element to produce those small injection masses. Currently, one of the requirements for HPDF engines is full-load diesel operation. This limits the smallest pilot masses.

Ammonia needs a great amount of activation energy to combust. The lower the energy the later starts the HRR. Higher injection pressure and higher fuel temperature have a positive effect on the HRR of the ammonia combustion. A greater pilot mass leads to an earlier ignition of the ammonia, but not necessary to a faster combustion.

Outlook

Ammonia is known for a high NOx production in combustion, especially when burned in lean combustion mode.[10] In the HPDF combustion, a SCR-system is mandatory – no matter which fuel combination, so this is no argument against the technology.

The fuels investigated are both suitable for use in HPDF-combustion processes. Both present special challenges in their application. In the future, the exhaust emissions of both fuels should be investigated in detail. This has not been done in this study, because of the used mechanism in the numerical model. The GRI Mech 3.0 is known, that it does not give correct NOx prediction for ammonia/air flames.[10] It has been used anyway because it gives good results for the burning velocities over a wide range of fuel/air ratios and the focus in this work was on ignition and flame propagation in the ammonia flame.

Because of the need of the decarbonisation of the transport sector, both fuels, hydrogen and ammonia will play a big role in future combustion systems, whereas the mixing-controlled HPDF-combustion is a fuel-flexible alternative to the classical diesel engines.

Acknowledgements

The project was carried out in collaboration with Woodward L'Orange and MTU Friedrichshafen. Their support is gratefully acknowledged. The authors also want to thank CONVERGE CFD for providing the software, licenses and technical support for the simulations.

Declaration of conflicting interests

The author(s) declared no potential conflicts of interest with respect to the research, authorship, and/or publication of this article.

Funding

The author(s) disclosed receipt of the following financial support for the research, authorship, and/or publication of this article: This study formed part of the "MethQuest-MethMare" project, which was funded by the German Federal Ministry of Economic Affairs and Energy.

ORCID iDs

Stephanie Frankl https://orcid.org/0000-0001-8414-4594
Maximilian Prager https://orcid.org/0000-0003-2507-6530

References

1. IPCC SYR TSU. Climate change 2014: synthesis report 2015.
2. Pavlenko N, Comer B, Zhou Y, Clark N and Rutherford D. The climate implications of using LNG as a marine fuel. Working paper 2020-02, 2020.
3. Imhof D. *Visual combustion studies for environmentally friendly marine diesel and gas engines*, Dissertation, Kyushu University, Kyushu, Japan, 2013.
4. Boog M, Dumser F, Berger I, Fink G, Jud M, Gleis S, et al. Entwicklung eines high pressure dual-fuel-konzepts für schnelllaufende drehzahlvariable Motoren in Schiffsantrieben. 11. Dessauer Gasmotorenkonferenz, 2019, Dessau.
5. McTaggart-Cowan GP, Jones HL, Rogak SN, Bushe WK, Hill PG and Munshi SR. The effects of high-pressure injection on a compression–ignition, direct injection of natural gas engine. *J Eng Gas Turbines Power* 2007; 129(2): 579–588.
6. Khosravi M, McTaggart-Cowan G and Kirchen P. Pyrometric imaging of soot processes in a pilot ignited direct injected natural gas engine. *Int J Engine Res*. Epub ahead of print 6 June 2020. DOI: 10.1177/1468087420919196.
7. Huang J, McTaggart-Cowan G and Munshi S. Large-eddy simulation of direct injection natural gas combustion in a heavy-duty truck engine using modified conditional moment closure model with low-dimensional manifold method. *Int J Engine Res* 2020; 21(5): 824–837.
8. NIST Chemistry WebBook. SRD 69, 2018. Fluid Properties of H2, CH4 and NH3.
9. Springer-Verlag GmbH. *VDI-Wärmeatlas: Mit 320 Tabellen. 11., bearb. und erw. Aufl.* Berlin: Springer Vieweg, 2013. (VDI-Buch).
10. Kobayashi H, Hayakawa A, Somarathne KDKA and Okafor EC. Science and technology of ammonia combustion. *Proc Combust Inst* 2019; 37(1): 109–133.
11. Boog M, Dumser F, Bärow E, Fink G, Jud M, Gleis S, et al. FlexDi - Flexible direkteinspritzende Motoren für die Schifffahrt. *Statustagung Maritime Technologien* 2018. D-52425 Jülich, www.fz-juelich.de/zb/openaccess (accessed 13 December 2018).
12. Senghaas C, Willmann M and Berger I. New injector family for high pressure gas and low caloric liquid fuels. In: *29th CIMAC Congress Vancouver 2019*, Vancouver, Canada, 10–14 June 2019.
13. Gleis S, Frankl S, Waligorski D, Prager M, Wachtmeister G, Prager D-IM, et al. Investigation of the High-Pressure-Dual-Fuel (HPDF) combustion process of natural gas on a fully optically accessible research engine. SAE technical paper 2019 // Investigation of the High-Pressure-Dual-Fuel (HPDF) combustion process of natural gas on a fully optically accessible research engine. SAE technical paper 2019.
14. Gleis S, Frankl S, Prager M and Wachtmeister G. Optical analysis of the combustion of potential future E-Fuels with a high pressure dual fuel injection system. In: *14th International AVL symposium on propulsion diagnostics*, Kurhaus, Baden-Baden, Germany, 23–24 June 2020.
15. Frankl S and Gleis S. Development of a 3D-CFD model for a full optical high-pressure dual-fuel engine. *SAE Int J Engines* 2020; 13(2): 2020.
16. Frankl S, Gleis S and Wachtmeister G. Interpretation of ignition and combustion in a full-optical High-Pressure-Dual-Fuel (HPDF) engine using 3D-CFD methods. In: *29th CIMAC Congress Vancouver 2019*, Vancouver, Canada, 10–14 June 2019.
17. International Organisation for Standardization. ISO 14687:2019: Hydrogen fuel quality - Product specification, 2019 2019-11.

18. European Space Agency. Vulcain engine, http://www.esa.int/Enabling_Support/Space_Transportation/Launch_vehicles/Vulcain_engine (accessed 13 February 2020).
19. Dimitriou P and Tsujimura T. A review of hydrogen as a compression ignition engine fuel. *Int J Hydrogen Energy* 2017; 42(38): 24470–24486.
20. Kiesgen G, Klüting M, Bock C and Fischer H. The new 12-cylinder hydrogen engine in the 7 series: the H2 ICE age has begun. In: *SAE 2006 World Congress & Exhibition*, Detroit, MI, 3–6 April 2006.
21. Herdin G, Gruber F, Klausner J, Robitschko R and Chvatal D. Hydrogen and hydrogen mixtures as fuel in stationary gas engines. SAE technical paper 2007-01-0012, 2007.
22. Rottengruber H, Wiebicke U, Woschni G and Zeilinger K. Wasserstoff-Dieselmotor mit Direkteinspritzung, hoher Leistungsdichte und geringer Abgasemission. Teil 3: Versuche und Berechnungen am Motor. *MTZ - Motortechnische Zeitschrift* 2000; 61: 122–128. https://link.springer.com/content/pdf/10.1007/BF03226557. pdf
23. Dawood F, Anda M and Shafiullah GM. Hydrogen production for energy: an overview. *Int J Hydrogen Energy* 2020; 45(7): 3847–3869.
24. Aarnes J, Eijgelaar M and Hektor EA. Hydrogen as an energy carrier: an evaluation of emerging hydrogen value chains, Hovik Norway, 11/2018, https://www.dnvgl.com/oilgas/download/thank-you/download-hydrogen-as-an-energy-noindex.html (accessed 20 February 2020).
25. Lan R, Irvine JTS and Tao S. Ammonia and related chemicals as potential indirect hydrogen storage materials. *Int J Hydrogen Energy* 2012; 37(2): 1482–1494.
26. Lamb KE, Dolan MD and Kennedy DF. Ammonia for hydrogen storage; A review of catalytic ammonia decomposition and hydrogen separation and purification. *Int J Hydrogen Energy* 2019; 44(7): 3580–3593.
27. Dimitriou P and Javaid R. A review of ammonia as a compression ignition engine fuel. *Int J Hydrogen Energy* 2020; 45(11): 7098–7118.
28. Kroch E. Ammonia - a fuel for motor buses. *J Inst Pet* 1945; 31: 213–223.
29. Pearsall TJ and Garabedian CG. Combustion of anhydrous ammonia in diesel engines. *SAE technical paper* 670947, 1967
30. Linde Gas GmbH. Sicherheitsdatenblatt Ammoniak, wasserfrei, 2013, https://produkte.linde-gas.At/sdb_konform/NH3_10021772DE.pdf (accessed 17 September 2020).
31. CONVERGE. Version 2.4. Convergent science, 2018, https://convergecfd.com/
32. Bowditch FW. A new tool for combustion research a quartz piston engine. *SAE technical paper* 610002, 1961.
33. Smith GP, Golden DM, Frenklach M, Moriarty NW, Eiteneer B, Goldenberg M, et al. GRI-Mech 3.0, http://combustion.berkeley.edu/gri-mech/version30/files30/grimech30.dat (accessed 7 January 2020).
34. Jud M, Wieland C, Fink G and Sattelmayer T. Numerical analysis of the combustion process in dual-fuel engines with direct injection of natural gas. In: *Proceedings of the ASME 2018 internal combustion fall technical conference*, San Diego, CA, 4–7 November 2018.
35. Jud M, Fink G and Sattelmayer T. Predicting ignition and combustion of a pilot ignited natural gas jet using numerical simulation based on detailed chemistry. In: *Proceedings of the ASME 2017 internal combustion engine division fall technical conference*, Seattle, Washington, 15–18 October 2017.
36. Han X, Wang Z, Costa M, Sun Z, He Y and Cen K. Experimental and kinetic modeling study of laminar burning velocities of NH3/air, NH3/H2/air, NH3/CO/air and NH3/CH4/air premixed flames. *Combust Flame* 2019; 206: 214–226.
37. Linstrom P. NIST chemistry webbook, NIST standard reference database 69: fluid data for ammonia, 1997, https://webbook.nist.gov/cgi/cbook.Cgi?Name = Ammonia&Units = SI (accessed 8 April 2020).
38. Mathieu O and Petersen EL. Experimental and modeling study on the high-temperature oxidation of ammonia and related NOx chemistry. *Combust Flame* 2015; 162(3): 554–570.
39. Reiter AJ and Kong S-C. Combustion and emissions characteristics of compression-ignition engine using dual ammonia-diesel fuel. *Fuel* 2011; 90(1): 87–97.

Appendix

Computational grid

Figure A1 shows exemplary the resulting grid for the hydrogen (left) and the ammonia (right) HPDF-combustion. The cylinder head as well as the liner and the piston have a boundary fixed embedding of scale 2.

For the liquid injection there is a 2-step fixed embedding. The cells close to the nozzle exit have a cell length of 0.0625 mm whereas the second embedding have a length of 0.125 mm. The minimum cell size resulting from AMR is 0.125 mm, as close to the gas injector. For the use of ammonia as main fuel, a conical fixed embedding, similar to the diesel fixed embedding is included into the domain. The inner cell

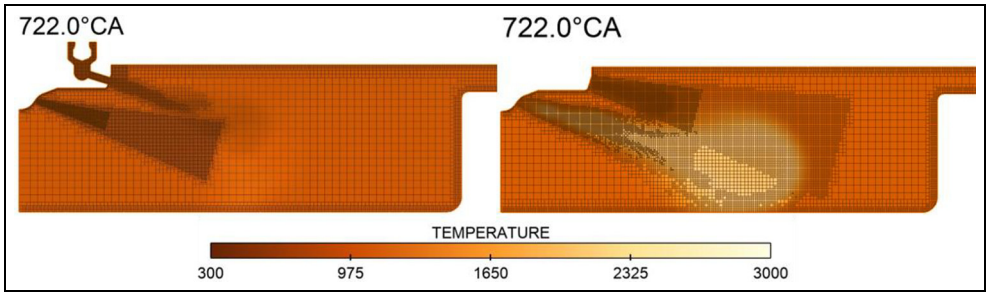

Figure A1. Resulting grid with two-step fixed embedding for the diesel pilot and adaptive mesh refinement for the hydrogen jet.

cone has cells of 0.125 mm length, the outer cone 0.25 mm length.

Definitions/Abbreviations

CA	Crank angle
CFD	Computational Fluid Dynamics
HPDF	High pressure dual fuel
HRR	Heat release rate
SCR	Selective catalytic reduction
SOI	Start of Injection
TDC	Top Dead Centre